Available online at www.sciencedirect.com
ScienceDirect
Journal of Catalysis 243 (2006) 239–251
JOURNAL OF CATALYSIS
www.elsevier.com/locate/jcat

Nanostructured Pd/C catalysts prepared by grafting of model carboxylate complexes onto functionalized carbon

S. Hermans [a], C. Diverchy [a], O. Demoulin [b], V. Dubois [c], E.M. Gaigneaux [b], M. Devillers [a,*]

[a] *Université catholique de Louvain, Unité de chimie des matériaux inorganiques et organiques, Place Louis Pasteur 1/3, B-1348 Louvain-la-Neuve, Belgium*
[b] *Université catholique de Louvain, Unité de catalyse et chimie des matériaux divisés, Croix du Sud 2/17, B-1348 Louvain-la-Neuve, Belgium*
[c] *Meurice Institute, Avenue Emile Gryzon 1, B-1070 Brussels, Belgium*

Received 22 May 2006; revised 13 July 2006; accepted 14 July 2006

Available online 6 September 2006

Abstract

Pd(5 wt%)/C catalysts were prepared by grafting carboxylate precursors onto functionalized carbon. The functionalization of the support was carried out with HNO_3 or H_2O_2, and the number and nature of oxygenated functions introduced were determined by a combination of simplified Boehm's titration, XPS, BET, and DRIFTS. These functions were then used as anchors for model Pd precursors through covalent bonding. The underlying ligand-exchange mechanism was elucidated through detailed XPS studies. The thermal activation of the grafted materials was followed by in situ mass spectrometry, which demonstrated that it consisted of ligand losses. The activated samples were characterized by SEM, XRD, CO chemisorption, and XPS and used in the reduction of 2-methyl-2-nitropropane (MNP) into *t*-butylamine (TBA). The catalytic activity was shown to be correlated with the initial carbon acidity and the Pd dispersion.

Keywords: Palladium; Carbon; Functionalization; Oxygenated functions; Heterogeneous catalysis; Hydrogenation; Grafting

1. Introduction

Carbonaceous materials are ideal supports for heterogeneous catalysts, because they are cheap, inert, and robust [1,2]. Moreover, the so-called "activated" (or "active") carbons present very high specific surface areas that allow high dispersion of the supported catalytically active phase [2]. The other advantages of carbon supports compared with inorganic oxides such as silica and alumina is that their surface favors the metallic reduced state and interface effects are minimized. In contrast, oxide supports present surface hydroxyl groups that stabilize oxidized phases and also are sensitive to harsh conditions, especially moisture. Consequently, many industrial processes make use of carbon-supported catalysts, especially for reactions carried out in the liquid phase [2]. However, the use of carbon materials as catalyst supports carries several major drawbacks. First, due to the variety of possible raw materials (e.g., coal, wood, peat, fruit stones, coconut shells) for producing active carbon and the various methods of carbonization used, its physicochemical characteristics vary greatly from one batch to the other [2–5]. Second, due to its high absorbing power (black body), carbon is not easily characterized spectroscopically by IR or Raman. Third, its inertness, which can be advantageous in some circumstances, becomes a disadvantage when trying to chemically modify its surface. Hence, the use of carbonaceous materials as catalyst supports rely mainly on preparation methods developed empirically.

The transformation of the raw material into a usable carbon support can be carried out in two ways: a physical or a chemical "activation" method [2,4,5]. In the latter case, the final high-surface area support is formed in one step by using a reactant for chemical activation such as zinc chloride, phosphoric acid, or potassium hydroxide. In the former case, the raw material is carbonized at high temperature (700–800 °C), followed by oxidative "activation" to increase the specific surface area by developing the pore system. In the final carbon material, hetero-atoms, such as O, N, or S, remaining from the source material are responsible for the surface acidic/basic character.

* Corresponding author. Fax: +32 10 47 23 30.
E-mail address: devillers@chim.ucl.ac.be (M. Devillers).

0021-9517/$ – see front matter
doi:10.1016/j.jcat.2006.07.019

Moreover, functional groups are also introduced at the surface in the process of creating the porosity [2,5]. These functions are present in modest amounts and can be removed by thermal treatment at high temperature [3,6–10]. In contrast, to increase the surface reactivity, the number of oxygenated functions can be increased by further oxidation in the gas or liquid phase [11]. The gas-phase treatments usually involve oxidation in a flow of air [12–15], O_2 (in N_2 or Ar) [8,9,16–22], N_2O (in N_2) [8] oxygen plasma [23–25], or ozone [25,26], whereas liquid-phase functionalization implies stirring a given amount of solid carbon in a solution of HNO_3 (see below), H_2O_2 (see below), $(NH_4)_2S_2O_8$ [16,23,24,27–30], NaOCl [13,16], $Ca(ClO)_2$ [31], or $KMnO_4$ [16,32], for example. The nature of the possible oxygen-containing groups present at the surface of an active carbon (before or after oxidative functionalization) has been determined to be mainly of the carboxylic, lactonic, phenolic, and carbonyl types [3,11,33]. Consequently, one can speak of a "surface acidity" for active carbons [11]. Boehm and coworkers have developed a method to quantify these functions by titration [3,11,16,33,34]. Oxygenated surface functions can also be characterized by FTIR or DRIFTS, TPD, XPS, TGA/MS, and other methods [1,6,8,14,22,31,34–39]. The point of zero charge (PZC) also has been shown to give a good indication of the acidic/basic properties of carbons and can be determined by, for example, mass titration [40].

The liquid-phase functionalization of active carbons with HNO_3 in particular has already been the object of many studies. Although gas-phase oxidation increases mainly the concentration of surface hydroxyls and carbonyls (as well as lactones and anhydrides), nitric acid treatment leads to a marked increase in carboxylic acid groups, as well as lactones to a lesser extent [3,7–9,13,14,18,20,29–31,41–44]. It was found that the number of oxygen functions introduced is dependent on the HNO_3 concentration used [45] (although one study reported an opposite effect [32]), or the temperature at which the treatment is carried out [6,46] and its duration [9]. Usually, the harsh oxidizing conditions associated with a HNO_3 treatment tend to modify the textural characteristics of the carbon used [27,39,43,47–52], but it has also been shown that O-groups can be introduced by HNO_3 under mild conditions (low concentration, temperature, and/or duration) without significantly modifying the porous structure [17,21,40,44,49,52,53]. Similarly, many authors have already carried out carbon oxidation with H_2O_2 and studied its particular effects, but less extensively than with nitric acid. The amount of surface O-groups introduced by H_2O_2 is generally lower than that introduced by HNO_3 [10,17,27,29,44,50,51,54,55]. It is possible to slightly augment the amount introduced by increasing the concentration of the H_2O_2 solution used [56]. The functions introduced are also acidic in nature, but are usually of lower strength (mainly lactones rather than carboxylic acids) [13,23,24,26,30,32], but, surprisingly, H_2O_2 was also found to be able to create new surface basic sites in addition to the acidic ones [30]. One paper reported the effect of pH control on H_2O_2 functionalization, leading to higher oxidative power [57]. In addition, it was found that H_2O_2 does not usually modify the textural characteristics of the treated carbon [25], although it has been shown to have an effect in some cases [23,24].

The present paper aims to show that it is possible to prepare carbon-supported catalysts in a controlled manner. Our strategy relies on the idea of introducing acidic functions in known amounts at the support's surface and then using them as anchors for grafting the catalytically active phase. In particular, using carboxylate complexes allows a ligand-exchange process for surface carboxylic groups, thus producing grafted molecular fragments of controlled structure. To go even further, we have used "probe" molecules containing chelate ligands and/or fluorine-containing fragments to model the chemical interaction of the metallic precursor with the prefunctionalized support. The presence of chelating ligands allows us to direct ligand substitution toward selective exchanges, whereas the introduction of F atoms provides a quantitative probe for XPS characterization. The present study aims to control precisely each step of the catalyst preparation, and via "molecular modeling" with "probe" molecules, to gain a precise picture of the fragments grafted onto the carbon supports. Studies dealing with real grafting of metallic species onto carbonaceous materials remain very scarce, and the methods used usually were not optimal [58]. One paper reported the use of a carbon-supported Pd complex that is simply adsorbed on the surface and remains intact and active for catalytic hydrogenation [59]. Ryndin et al. used oxidized diamond to anchor the organometallic complex $[(C_3H_5)Pd(C_5H_5)]$ and found that the resulting Pd particles after reduction are extremely small (<10 Å) and resistant to sintering [60]. Immobilization of metal complexes on a carbon electrode via their ligands was also carried out through electrochemical cation radical formation [61]. Recent reports by Silva et al. presented successful carbon-grafted complexes, even chiral ones in some cases, such as manganese(III) *salen* species, for applications in (enantioselective) epoxidation, for example [62–65]. Another recent work by another group [66] used HNO_3-functionalized carbon to covalently attach acetylacetonate complexes for application in liquid-phase oxidation. In both these recent cases, the stability toward leaching of the complexes into the catalytic reaction medium was very good.

Our strategy was used to prepare Pd(5 wt%)/C catalysts, the performance of which was evaluated (after thermal activation) in the selective hydrogenation of 2-methyl-2-nitropropane (MNP) into *t*-butylamine (TBA) (Scheme 1). The hydrogenation of nitro compounds to the corresponding amines is an interesting reaction from an industrial standpoint, because these chemicals are used as basic raw materials for urethanes, rubber chemicals, dyes, and pharmaceuticals [2]. Although the catalytic hydrogenation of aromatic nitro compounds has been studied extensively, far fewer studies have been devoted to the transformation of aliphatic nitro compounds into the corresponding amines [67–70]. Previous reports on nitropropane or nitrobutane reduction have shown that Pd/C catalysts display interesting performance [68–70] and that the surface state of the support might have an influence on the catalytic activity [70]. The literature reports that in general (and for other reactions), the augmentation of oxygenated surface groups in the carbon support could have a double impact in catalysis: (i) via a sim-

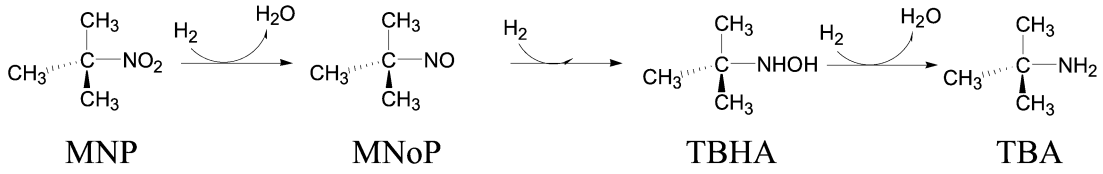

Scheme 1. Reduction of 2-methyl-2-nitropropane (MNP) into *t*-butylamine (TBA).

ple dispersion effect, when support functionalization leads to higher metallic dispersions and hence higher activity [20,26,45,53,71], or (ii) by a more complicated mechanism in which the O-functions play an active role in the catalytic reaction (e.g., as adsorption sites) [9,70,72]. In addition to the fact that the introduction of O-functions provides anchoring sites for catalyst precursor adsorption and thus the potential for high dispersion, it also changes the surface charge in some pH windows (hence the precursor–surface interactions) [34,73] and the surface hydrophobic nature [13]. Moreover, the final dispersion also might be influenced by the thermal stability of the O-functions introduced [34,73].

2. Experimental

2.1. Materials

The activated carbon used, called SX+ (acid-washed steam activated carbon, ash content: 6%; $S_{BET} = 922$ m^2/g; $S_{BJH} = 245$ m^2/g; pore volume [BJH] = 0.41 cm^3/g), was supplied by NORIT and sieved to keep only the fraction of granulometry at 50–100 μm. It was submitted to oxidation treatments in the liquid phase, with HNO_3 [1 mol/L; Aldrich, conc. Acros, p.a.] or H_2O_2 [Acros, 35 wt% solution] (each time with 50 mL of reagent for 2 g of SX+), under variable conditions of reactant concentration, duration, and temperature, as specified in the Results section. After treatment, the functionalized carbon was filtered out, washed with distilled water on a Soxhlet apparatus for 24 h, and dried under vacuum in an oven at 70 °C for 4 h.

Carbon-supported palladium catalysts were prepared using carboxylate palladium complexes as precursors. The selected complexes were synthesized as reported in the literature and described below. Diacetato(2,2′-bipyridine)palladium (II) [$Pd(OAc)_2$(bipy)] was synthesized from palladium acetate [Rocc, Pd 47.27%] and 2,2′-bipyridine [Acros, 99+%] in acetone [Fisher Chemicals, 99.99%] as described previously [47,74] (yield: 90%). IR (KBr disk): ν_{as}(COO) 1625, ν(CN) 1578, ν_s(COO) 1369 cm^{-1}. Elemental analysis: anal. (calcd.): C: 40.82 (44.17), H: 3.98 (3.71), N: 6.46 (7.36). MS (ESI$^+$): m/z 321.0 [Pd(OAc)(bipy)]$^+$, 293.8 [Pd(OAc)(bipy-HCN)]$^+$, 262 [Pd^I(bipy)]$^+$, 157.2 [bipy+H$^+$]$^+$. A second complex, (2,2′-bipyridine)bis(trifluoroacetato)palladium (II) [$Pd(CF_3COO)_2$(bipy)], was obtained by ligand exchange [47], using the synthesized [$Pd(OAc)_2$(bipy)] and trifluoroacetic acid [Acros, 99%] as reactants (yield: 71%). IR (KBr disk): ν_{as}(COO) 1685, ν_s(COO) 1425 cm^{-1}. Elemental analysis: anal. (calcd.): C: 34.24 (34.41), H: 1.44 (1.65), N: 5.00 (5.73). MS (ESI$^+$): m/z 375.0 [$Pd(O_2CCF_3)$(bipy)]$^+$, 292.9 [$Pd(O_2CCF_3)$(py)]$^+$, 222.9 [$Pd(O_2CCF_3)$]$^+$, 157.2 [bipy+H$^+$]$^+$. Diacetato bis(diethylamine) palladium (II) [$Pd(OAc)_2$-$(Et_2NH)_2$] resulted from direct reaction of palladium acetate [Rocc, Pd 47.27%] with diethylamine [Acros, 99+%] [74–76] (yield: 66%). IR (KBr disk): ν(NH) 3120, ν_{as}(COO) 1586, ν_s(COO) 1375, ν(CN) 1150, ν(CN) 869, δ(OCO) 686, ω(COO) 611, ρ(COO) 543, ν(Pd-ligand) 441 cm^{-1}. Elemental analysis: anal. (calcd.): C: 38.89 (38.87), H: 7.69 (7.61), N: 7.52 (7.56). MS (EI$^+$): m/z 249.6 [$Pd(Et_2NH)_2^{2+}$–H$^+$]$^+$, 176.6 [$Pd(Et_2NH)^{2+}$–H$^+$]$^+$, 72.0 [Et_2NH–H]$^+$, 57.9 [Et_2NH–CH_3]$^+$, 44.0 [Et_2NH–CH_3CH_2]$^+$.

The synthesized complexes were then grafted onto the various samples of treated carbon supports under the following conditions. The complex was dissolved in water and stirred with a fixed amount of carbon at room temperature (unless otherwise stated) for 24 h. The two bipyridine complexes were used in equimolar ratios with respect to the amount of acid functions on the carbon sample used, as determined by Boehm's titration (see Section 2.2.1), starting from 1 g of active carbon in 50 mL of distilled water. This would correspond to 3–15 wt% Pd loading in a final activated carbon-supported material. The amounts for grafting of [$Pd(OAc)_2(Et_2NH)_2$] were calculated to get Pd(5 wt%)/C catalysts (0.1742 g of complex and 0.95 g of active carbon in 50 mL of distilled water). The grafted materials were then separated by filtration, abundantly washed with water, and dried under vacuum in an oven at 70 °C for 4 h. The filtrate was kept for further analysis by atomic absorption spectrometry using a Perkin–Elmer 3110 spectrometer fitted with a flame atomizer (after realization of a calibration curve from 1 to 10 mg/L with standard solutions obtained by dilution of a 1 g/L palladium solution from Acros).

The grafted materials thus obtained were submitted to thermal activation in a Carbolite tubular oven under nitrogen and eventually hydrogen flow. The conditions of temperature and duration of activation were varied to optimize the metallic dispersion and are detailed in Section 3.

2.2. Characterization methods

2.2.1. Boehm's titration

The titration method developed by Boehm et al. [3] was implemented to assess the amount of acidic functions on the carbon surface of the treated support samples. This method involves neutralization of the surface acid functions with excess amounts of selected bases, followed by back titration with hydrochloric acid [3]. In this study, only sodium hydroxide was used as a base, which allows the neutralization (hence quantification) of the sum of all phenol, lactone, and carboxylic acid groups, leading to a value hereinafter termed "total acidity"

(in mmol/100 g of carbon). In a typical experiment, 50 mL of NaOH 0.05 mol/L [FIXANAL, Riedel-de-Haën] is brought into contact with 0.7 g of carbon, and the mixture is stirred for 24 h at room temperature. The carbon is then filtered out, and the filtrate is titrated with hydrochloric acid, using phenolphthalein as an indicator. All of these steps are carried out under nitrogen flushing, using freshly distilled decarbonated water.

2.2.2. Characterization of carbonaceous materials

X-ray photoelectron spectroscopy (XPS) was carried out on a SSI-X-probe (SSX-100/206) Fisons spectrometer. The powder samples were pressed on small troughs using double-face adhesive tape and then placed on an insulating homemade ceramic sample holder (Macor, Switzerland). A nickel grid was fixed above the samples, and an electron flood gun was set at 8 eV to overcompensate for the positive charging of the samples during the analyses. The analyzed area was approximately 1.4 mm^2, and the pass energy was set at 150 eV. Under these conditions, the resolution determined by the full width at half maximum (FWHM) of the $Au4f_{7/2}$ peak of a clean gold reference sample was around 1.6 eV. Calibration of the energy scale was done with reference to the $Au4f_{7/2}$ peak at 84 eV, and the binding energies were set by fixing the C1s peak [C–(C,H) component] at 284.8 eV. Three photopeaks (C1s, O1s, and N1s) were systematically analyzed for the carbonaceous materials. The F1s peak was taken into account if necessary, and the Pd3d peak was added for the catalysts. The XPS results were decomposed with the CasaXPS software using a sum of Gaussian/Lorentzian (85/15) after subtraction of a Shirley-type baseline. The constraints used for decomposition of the Pd3d peak were as follows: imposing an area ratio $Pd3d_{5/2}/Pd3d_{3/2}$ of 1.5, a difference in the binding energies ($Pd3d_{3/2}$–$Pd3d_{5/2}$) of 5.26 eV, and a FWHM ratio (for the $Pd3d_{5/2}/Pd3d_{3/2}$ peaks) of 1.

DRIFTS studies were conducted with a Bruker Equinox 55 spectrometer accumulating 5000 scans per spectrum with a resolution of 4 cm^{-1}. The detector was of the MCT type. The cell was coupled with a Balzers QMS 200 mass spectrometer. The samples were first degassed under helium flow (30 mL/min) for 1 h at room temperature, in a commercial cell (Spectra-Tech 0030-102) built in the spectrometer. DRIFTS spectra of functionalized carbon materials were taken at 120 °C to avoid obstruction of the spectra by H_2O. Mass spectra of the grafted samples were recorded using a heating ramp of 2 or 3 °C/min.

The specific surface areas were measured on a Micromeritics ASAP 2000 instrument by nitrogen adsorption at −196 °C (77 K). Before analysis, the sample (0.1 g) was degassed for several hours at 150 °C under 4 mm Hg pressure.

Metallic dispersion measurements were conducted by CO chemisorption with a Pulse Chemisorb 2700 apparatus from Micromeritics. The sample (about 30 mg) was first reduced under hydrogen flow (30 mL/min) at 150 °C for 1 h, then swept by a helium flow (30 mL/min) at 200 °C for 2 h. The sample was finally brought back to room temperature, at which point it was subjected to a sequence of CO pulses. The metallic dispersion was calculated from the cumulative amount of adsorbed CO (i.e., the sum of nondetected CO in each pulse), following

$$D = \frac{V_{\mathrm{NTP}} M}{V_{\mathrm{M}} m C P} \times 100,$$

where D is the metallic dispersion (%), V_{NTP} is the adsorbed volume under normal temperature and pressure conditions, M is the atomic weight of the metal (here Pd), V_{M} is the molar volume (22.414 L/mol) of the active gas at normal conditions (0 °C, 1 atm), m is the dry sample mass, C is the stoichiometric coefficient for CO adsorption on Pd (a 1:1 stoichiometry was used in the present study), and P is the wt% of metal in the sample (here 5).

Topographic SEM images were obtained using a FEG Digital Scanning (DMS 982 Gemini LEO) electron microscope fitted with an EDAX analyzer (Phoenix CDU LEAP). Samples were stuck using double-face adhesive tape on 5-mm-diameter aluminum specimen stubs from Agar Scientific.

XRD powder analyses were conducted using a Siemens D5000 diffractometer equipped with a copper anticathode ($\lambda_{K\alpha} = 154.18$ pm). The samples were supported on Si monocrystals and analyzed at 15–80° with increments of 0.03° per 4 s. The detected phases were identified by reference to the JCPDS database. The metal loading in the activated samples was determined via ICP-AES (Medac, Egham, UK).

2.2.3. Characterization of the Pd complexes

The IR spectra were obtained using a FTIR spectrometer (Bio-Rad FTS 135) at a resolution of 4 cm^{-1} with KBr pellets containing 1 wt% of the complexes. The three synthesized complexes were characterized for C–H–N elemental content by the microanalysis service of University College, London.

Thermograms were recorded on a Mettler Toledo 851^e TGA system under a 100 mL/min nitrogen flow at a heating rate of 10 °C/min, between 20 and 500 °C. The sample (∼3 mg) was placed in an alumina container (70 μL).

A LCQ FINNIGAN MAT or a TSQ 7000 FINNIGAN MAT mass spectrometer was used to analyze the complexes using electrospray (ESI) and electronic impact (EI) ionization methods, respectively.

2.3. Catalytic tests

The reaction used for the catalytic tests is the reduction of 2-methyl-2-nitropropane (MNP) into *t*-butylamine (TBA) (Scheme 1). The tests were carried out in a steel Parr 4521 reactor fitted with a temperature control device and a mechanical stirrer fixed at 2500 rpm. In these conditions, extragranular diffusion limitations are avoided and a kinetic regime is guaranteed [70]. First, 375 mL of methanol (Fluka, p.a. >99.8%), a known quantity (about 0.3 g) of catalyst, and 3 mL of 1-propanol (chromatographic internal standard; Acros, p.a. >99%) were poured into the reactor and degassed for 15 min under nitrogen. The mixture was then submitted to pretreatment at 80 °C for 1 h, under 17 bar of H_2. The reactant (MNP; Alfa Aesar, 99%) was dissolved in 25 mL of methanol and degassed (under N_2) before being added into the reactor. During catalytic reaction, the reactor was kept under a pressure of about

12 bar H_2 and a temperature of 60 °C. Sampling of the reaction mixture took place at regular time intervals, and the product distribution was obtained by gas chromatography; further details have been provided previously [70].

The chromatograph was an Agilent Technologies 6890N fitted with a WCOT fused silica Chrompack CP-WAX 52 CB capillary column (length, 50 m; internal diameter, 0.53 mm; film thickness, 2 μm). The vector gas was He (50 kPa), and the temperature of the injector and detector was maintained at 250 °C. The samples were automatically injected via a split–splitless injector with a split flow of 20 mL/min. The temperature program for analysis was as follows: 120 °C for 5 min, heating to 230 °C (30 °C/min), isotherm at 230 °C. The signal received by a FID detector was directly interpreted by a computer using the HP Chemstation software. The surface area of each peak was converted into concentration by applying the response factor with respect to the internal standard.

The specific activity measured can be expressed by either the rate of MNP conversion or the rate of TBA formation. In this study, the catalysts are compared on the basis of the former, because an apparent zero-order is always observed; hence the slope is proportional to the catalyst amount. The presented results are normalized with respect to the mass of catalyst used.

3. Results and discussion

3.1. Functionalization of SX+ carbon

The functionalization of SX+ carbon was carried out under various conditions. The concentration (0.25–2.5 mol/L), temperature (room temperature to reflux), and duration (1–72 h) were varied for the oxidative treatments with HNO_3, whereas the concentration (0.2 or 11.68 mol/L) and duration (1–24 h) were varied for treatments with H_2O_2. The support was characterized by several methods to evaluate the extent of functionalization. Boehm's titrations and XPS were used to quantify the obtained acidity, whereas DRIFTS was applied to determine the nature of the introduced oxygenated functions. In addition, the textural state of the modified supports was explored through BET.

The results of Boehm's titrations presented in Table 1 show that the unmodified SX+ carbon (line 1 in Table 1) has some acid functions on its surface. Any treatment with HNO_3 or concentrated H_2O_2 provokes an increase in the number of surface oxygenated groups. The formation and relative quantities of these groups were influenced by the nature and concentration of the reactant used, as well as by the temperature and duration in cases of treatment with HNO_3. It appears that treatment with HNO_3 (lines 2–20) has a greater effect on total acidity than a treatment with H_2O_2 (lines 21–26), as mentioned in the literature [10,17,27,29,44,50,51,54,55]. Moreover, with HNO_3, temperature and concentration seem to have more effect than duration on the total acidity. More precisely, increasing the temperature to 50 °C (lines 7–9) did not have a major influence, but heating under reflux (lines 10–14, 17, 18, and 20) considerably enhanced the surface acidity. The effects of HNO_3 concentration [45] and treatment temperature [6,46] on the number of oxygen functions introduced have also been reported previously.

Table 1
Functionalization of SX+ carbon with HNO_3 or H_2O_2

	Treatment		Total acidity[b] (mmol/100 g C)	XPS O/C	BET (m^2/g)
	Temperature[a]	Duration (h)			
Unmodified SX+ carbon					
1	–	–	32.0	0.041	922
HNO_3 0.25 mol/L					
2	RT	1	56.9	0.054	
3	RT	24	67.4	0.050	916
4	RT	24	60.2	0.054	
5	RT	48	58.7	0.052	
6	RT	72	56.9	0.052	
7	50 °C	1/2	55.9	0.052	
8	50 °C	1	51.3	0.049	
9	50 °C	24	71.1	0.065	878
10	Reflux	1	80.1	0.063	
11	Reflux	24	138.5	0.12	
12	Reflux	24	135.8	0.099	913
13	Reflux	24	119.1	0.094	
14	Reflux	24	131.0	0.085	
HNO_3 1 mol/L					
15	RT	24	57.9	0.057	
16	RT	24	66.6	0.066	905
17	Reflux	24	254.7	0.16	793
18	Reflux	24	231.0	0.13	
HNO_3 2.5 mol/L					
19	RT	24	75.0	0.073	897
20	Reflux	24	325.6	0.19	756
H_2O_2 0.2 mol/L					
21	RT	1	28.6	0.047	
22	RT	8	32.5	0.048	
23	RT	24	32.5	0.047	927
H_2O_2 11.68 mol/L					
24	RT	1	48.7	0.058	
25	RT	8	52.9	0.059	
26	RT	24	48.4	0.055	904

[a] RT = room temperature.
[b] Determined by Boehm's titration.

These titration results were confirmed by determination of O/C surface ratios by XPS (Table 1). As expected, an increase in acidity (as determined by Boehm's titrations), corresponding to an increase in surface oxygenated functions, was related to higher O/C ratios (measured by XPS). More specifically, a linear correlation (Fig. 1) was found between the total acidity measured by Boehm's titration and the XPS results (O/C surface ratios). For most of the samples, the N1s zone contained no signal, indicating that no residue of nitric acid remained on the carbon. Reproducibility and repeatability were verified for both Boehm's titration and XPS.

The unmodified SX+ carbon has a BET surface area of about 922 m^2/g. When treated with HNO_3, its specific surface tends to decrease slightly, especially at high temperatures and concentrations (Table 1). This finding is in agreement with the literature, because it has already been shown that liquid-phase HNO_3 oxidation of carbon does not significantly modify its textural properties [17,21,40,44,49,52,53], except for severe

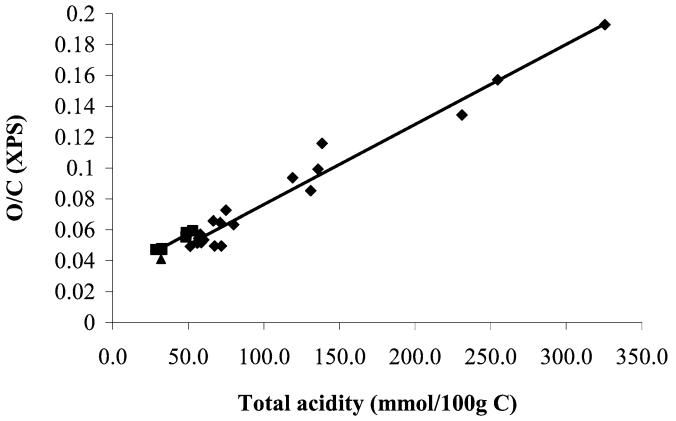

Fig. 1. Linear correlation found between XPS results (O/C surface ratios) and total acidity (measured by Boehm's titration) for carbons modified with HNO_3 (◆) or H_2O_2 (■) and unmodified SX+ carbon (▲).

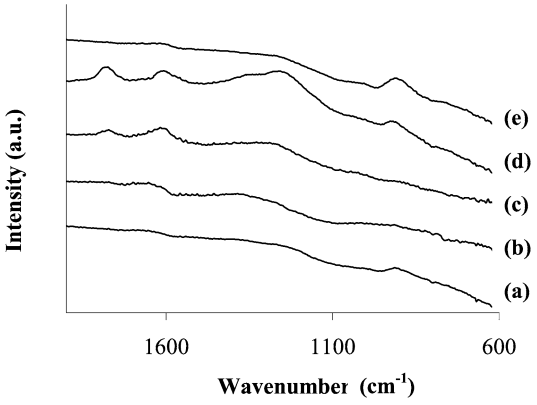

Fig. 2. DRIFTS spectra for (a) unmodified SX+ carbon, (b) C treated with HNO_3 0.25 mol/L under reflux, (c) C treated with HNO_3 1 mol/L under reflux, (d) C treated with HNO_3 2.5 mol/L under reflux, and (e) C treated with H_2O_2 11.68 mol/L. (Note: to allow comparisons, the duration of all treatments here was taken as 24 h.)

treatments [27,39,43,47–52]. Table 1 shows also that modification with H_2O_2 brought no change in specific surface area, again in agreement with the literature [25].

Five DRIFTS spectra of carbons with radically different acidities were recorded. These spectra display (as shown in Fig. 2) large bands attributable to the oxygenated functions. Although there is no general consensus in the literature, the assignment of the main IR bands associated with O-groups in functionalized carbons is summarized in Table 2 [1,6,8,23, 38,52]. The spectrum for the unmodified carbon showed weak bands at around 1600, 1200, and 900 cm^{-1}, corresponding to ν(C=O), ν(C–O), and ν(C–O) or ν(CO–O–CO), based on the assignments shown in Table 2. An increase in the oxygen content was clearly visible when the carbon was modified with HNO_3; the bands grew and lengthened, and a new band appeared at 1800 cm^{-1} [ν(C=O)]. This was expected, because nitric acid treatment is known to increase mainly the amount of carboxylic acid groups on carbon surfaces [3,7–9,13,14,18,20, 29–31,41–44]. The spectrum of the carbon modified with H_2O_2 was identical to that of SX+ apart from the amplification of the band at 900 cm^{-1}—not surprisingly, because H_2O_2 oxidation

Table 2
IR (main bands) of functionalized carbons

Wavenumber (cm^{-1})	Functions
1850–1700	ν(C=O): anhydride, lactone, ketone, carboxylic acid
1650–1550	ν(C=O): quinone, amide, carboxylate ν(C=C): aromatics
1450–1150	ν(C–O): ether, carboxylic acid, ester, lactone, phenol
950–850	ν(C–O): cyclic ether ν(CO–O–CO): aromatic cyclic anhydride (5-membered) δ(OH): carboxylic acid ν(O–O): peroxide

usually creates weak acid sites rather than carboxylic acids on the surface [13,23,24,26,30,32].

To summarize, the treatment of SX+ carbon with H_2O_2 brought about a smaller increase in the oxygenated surface groups than with HNO_3. Moreover, the nature of introduced groups was variable depending on the reactant. The most highly functionalized material (with HNO_3 2.5 mol/L, for 24 h under reflux) displayed a total acidity of 325.6 mmol/100 g and only a slightly smaller surface of ∼700 m^2/g, corresponding to 2.8 functions/nm^2. This compares well with previous studies in which values up to 1–3 acidic groups/nm^2 were found for highly oxidized carbon nanofibers [77].

3.2. Grafting of Pd complexes onto functionalized carbon

The oxygenated functions introduced on the support were used as anchors for the grafting of the synthesized metallic precursors. The grafting mechanism, consisting of ligand exchange, was first studied using [$Pd(OAc)_2$(bipy)] and [$Pd(O_2CCF_3)_2$(bipy)]. Then Pd(5 wt%)/C catalysts were prepared using [$Pd(OAc)_2(Et_2NH)_2$].

3.2.1. Synthesis and characterization of the complexes

The compounds [$Pd(OAc)_2$(bipy)], [$Pd(O_2CCF_3)_2$(bipy)], and [$Pd(OAc)_2(Et_2NH)_2$] were prepared as described in the literature [47,74,75], and characterized by IR, elemental analysis, TGA, and mass spectrometry. In their IR spectra, the ν_s(COO) and ν_{as}(COO) bands were particularly interesting, because the separation between them ($\Delta\nu_{(as\text{-}s)}$) varied with the coordination mode of carboxylate ligands [78]: $\Delta\nu_{(as\text{-}s)} \approx 150\ cm^{-1}$ for a chelating and $\Delta\nu_{(as\text{-}s)} > 200\ cm^{-1}$ for an unidentate coordination mode. These considerations allowed us to determine that in the starting complex [$Pd(OAc)_2$], both acetate ligands are coordinated in a chelating mode, whereas they become unidentate in the three synthesized complexes [$Pd(O_2CR)_2$(L)] (O_2CR = carboxylate, L = bipy or $(Et_2NH)_2$), in agreement with the literature [47,74–76,78].

Results from TGA analyses of the synthesized complexes, carried out under nitrogen, are given in Table 3. The comparison between calculated and experimental mass losses indicates that on heating, the complex [$Pd(OAc)_2(Et_2NH)_2$] lost all of its ligands. In contrast, the ligands loss for bipyridine complexes was not complete, probably due to the polyaromatic nature of

Table 3
TGA analyses of the synthesized Pd complexes (under nitrogen)

Complex	Calculated mass loss (%)		Experimental mass loss (%)	Final decomposition temperature (°C)
	Based on a PdO residue	Based on a Pd residue		
$[Pd(OAc)_2(bipy)]$	67.8	72.0	59.7	240
$[Pd(O_2CCF_3)_2(bipy)]$	74.9	78.2	46.1	270
$[Pd(OAc)_2(Et_2NH)_2]$	67.0	71.3	73.3	170

the bipy ligand. These observations justified our choice to use $[Pd(OAc)_2(Et_2NH)_2]$ only as a catalyst precursor.

The mass spectra recorded for each Pd compound show peaks corresponding to representative fragments arising from losses of ligands or fragments of them, as well as proton addition, and high mass entities corresponding to dimers, trimers, and lightly bound adducts.

3.2.2. Grafting of $[Pd(OAc)_2(bipy)]$ or $[Pd(O_2CCF_3)_2(bipy)]$ onto functionalized carbon

The advantages of these two complexes were linked to their solubility in water and the ease of interpretation because they presented nitrogen (and fluorine) atoms. But these complexes also had a disadvantage—results from TGA analysis showed that they could not be used for catalysis if thermal activation was used, because the bipyridine ligands could not be completely removed on heating. For these reasons, these complexes were used only to investigate the grafting mechanism of carboxylate complexes onto functionalized carbon.

The procedure for grafting $[Pd(O_2CR)_2(bipy)]$ compounds on carbon samples containing surface oxygenated functions is believed to proceed via substitution of the carboxylate ligands by surface –COOH groups according to a ligand-exchange mechanism. Among the possible resulting structures, one was thought to be the most probable (Scheme 2). Indeed, the presence of a N-donor chelating ligand limits the number of possible reactions by favoring substitution of the carboxylate ligands. This hypothesis was confirmed by XPS (see below).

A series of samples was prepared by reacting various batches of functionalized carbon with equimolar quantities of complex

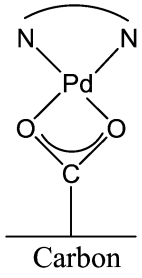

Scheme 2. Most probable grafting model for $[Pd(O_2CR)_2(bipy)]$ complexes onto functionalized carbon.

with respect to the amount of acid functions determined by titration. The influence of the initial carbon acidity, as well as the effect of the temperature during the grafting procedure, were studied. Table 4 shows that the higher the initial carbon acidity, the more the experimental Pd/C ratio differed from the calculated Pd/C value. This means that at high loading, all of the palladium introduced was not quantitatively grafted, due to a saturation effect of the acid functions, perhaps related to their proximity. These results were confirmed by atomic absorption analysis of the filtrates (last column of Table 4), which showed that some residual Pd remained in solution at high loading. When raising the grafting temperature (Table 4, compare lines 5, 6, and 7), the experimental XPS Pd/C ratios increased slightly, but the percentage of introduced Pd (measured by atomic absorption analysis of the filtrates) diminished. Thus, it seems that increasing the temperature allowed better dispersion (higher surface Pd concentration) but was detrimental to the total amount adsorbed. The Pd/N ratios were close to 0.5 in

Table 4
Grafting of $[Pd(OAc)_2(bipy)]$ (1 to 7) or $[Pd(O_2CCF_3)_2(bipy)]$ (8 and 9) on SX+ carbon and carbon functionalized with HNO_3

	Initial carbon acidity (mmol/100 g C)	Grafting		Pd/N (XPS)	Pd/C × 100 (XPS)		Relative amount of Pd adsorbed on C (%)[d]
		Temperature[b]	Duration (h)		Calculated[c]	Experimental	
1	32.0	RT	24	0.52	0.38	0.41	99.99
2	60.2	RT	24	0.65	0.72	0.74	99.28
3	138.5	RT	24	0.65	1.66	1.29	70.39
4[a]	138.5	RT	24	0.65	1.66	1.19	–
5	135.8	RT	24	0.62	1.63	1.02	84.03
6	135.8	50 °C	24	0.60	1.63	1.14	73.32
7	135.8	100 °C	24	0.74	1.63	1.38	66.95
8	138.5	RT	24	0.65	1.66	1.26	62.04
9[a]	138.5	RT	24	0.61	1.66	1.05	–

[a] Samples washed thoroughly with distilled water in a Soxhlet apparatus after the grafting procedure.
[b] RT = room temperature.
[c] Values calculated by considering 100% grafting of the Pd complex.
[d] The amount of nonadsorbed Pd was measured in the synthesis filtrates by atomic absorption, which allowed to calculate the amount of adsorbed Pd by difference (here expressed in terms of % of amount introduced initially).

most cases, confirming the hypothesis that the acetate ligands were exchanged for surface groups during the grafting procedure, while the bipyridine ligand remained linked to the palladium, as shown in the model displayed in Scheme 2. The Pd/N ratio became significantly higher for sample 7 (grafted under reflux), suggesting that the bipyridine ligand was more easily exchanged (or even destroyed) at higher temperature. Hence, in the remainder of this study, the grafting temperature was fixed at room temperature only.

Comparing the results obtained for samples 3 and 4 (Table 4) indicated that the palladium species was really bound chemically on the carbon surface, because the XPS values after thorough washing in a Soxhlet apparatus varied very little. In the same way, grafting of $[Pd(O_2CCF_3)_2(bipy)]$ was carried out to confirm that chemical links between the palladium complex and the carbon support could be achieved. Samples 8 and 9 gave rise to F/Pd ratios of 0.57 and 0.19, respectively. Thus, the F/Pd ratio decreased with abundant washing, but the Pd/C and Pd/N ratios remained very close in these two samples (Table 4), indicating that the "Pd(bipy)" fragment was actually grafted, whereas the exchanged trifluoroacetate ligands remained adsorbed on the surface in sample 8 and could be washed out in sample 9.

3.2.3. Grafting of $[Pd(OAc)_2(Et_2NH)_2]$

The complex $[Pd(OAc)_2(Et_2NH)_2]$, according to its crystal structure [79], is obtained predominantly in the *trans* form. This could preclude a clean carboxylate-exchange grafting mechanism, as the N-donor ligands (being nonchelating) are also potentially substituted. Due to its neat TGA and elemental analysis, the complex was nevertheless used to prepare Pd(5 wt%)/C catalysts using functionalized carbon samples of various acidities. The results obtained after grafting are summarized in Table 5. Low Pd/C ratios were obtained. To explore a possible evolution of the Pd dispersion with the carbon acidity, CO chemisorption measurements were implemented after activation (see below). The Pd/N ratios measured on the surface after grafting of $[Pd(OAc)_2(Et_2NH)_2]$ were variable, indicating that the ligand-exchange reactions were not as selective as for $[Pd(OAc)_2(bipy)]$ or $[Pd(O_2CCF_3)_2(bipy)]$. Here several exchange mechanisms are plausible, leading to different surface structures, as presented in Scheme 3. Based on the measured Pd/N ratios, hypothesis (a) was believed to be the predominant model. Other schemes are also possible—for example, taking into account an exchange mechanism involving two surface acidic functions or the occurrence of a *cis*/*trans* rearrangement in solution, leading to grafted fragments such as those shown in Scheme 3b or 3c.

Table 5
Grafting of $[Pd(OAc)_2(Et_2NH)_2]$ onto SX+ and functionalized carbon samples

	Initial carbon acidity (mmol/100 g C)	XPS		Relative amount of Pd adsorbed on C (%)[d]
		Pd/N	Pd/C (×100)	
1[a]	32.0	1.01	0.68	99.39
2[b]	72.0	1.42	0.62	99.47
3[b]	119.1	0.98	0.82	99.45
4[b]	254.7	0.65	0.90	99.71
5[b]	325.6	0.47	0.81	100.00
6[c]	52.9	1.04	0.71	99.83

[a] Nonfunctionalized carbon.
[b] C sample functionalized with HNO_3.
[c] C sample functionalized with H_2O_2.
[d] The amount of nonadsorbed Pd was measured in the synthesis filtrates by atomic absorption, which allowed to calculate the amount of adsorbed Pd by difference (here expressed in terms of % of amount introduced initially). In this case, 100% of palladium introduced corresponds to a final activated catalyst with a 5 wt% Pd loading.

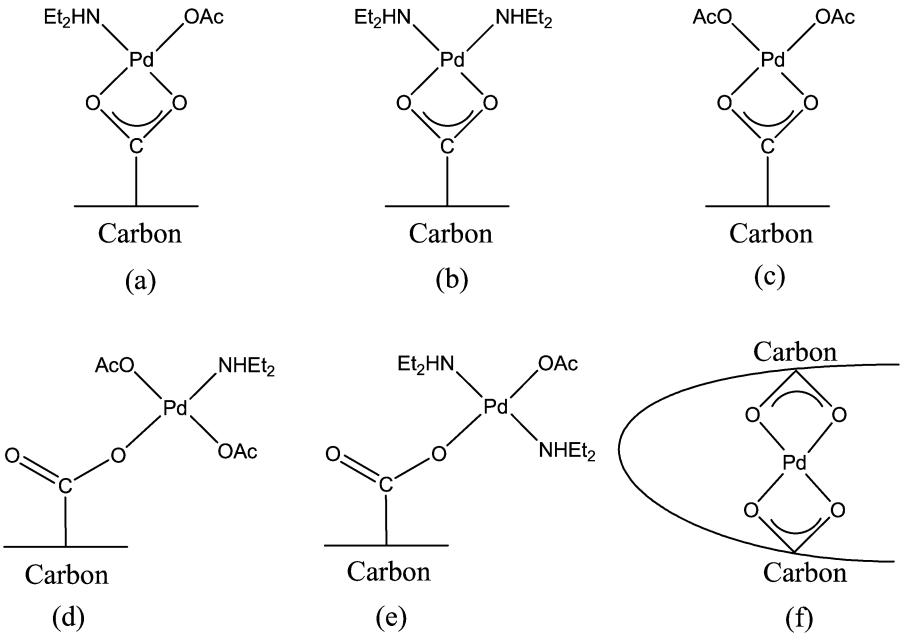

Scheme 3. Possible models for grafting of $[Pd(OAc)_2(Et_2NH)_2]$ onto functionalized carbon: (a) exchange of one acetate and one diethylamine ligands for a surface –COOH group, (b) exchange of two acetate ligands, (c) exchange of two diethylamine ligands, (d) exchange of one diethylamine only, (e) exchange of one acetate only, (f) exchange of all four ligands for two –COOH groups inside a pore. Models (b) and (c) imply the occurrence of a *cis*/*trans* rearrangement of the complex.

The Pd loading obtained by atomic absorption analysis of the filtrates, shown in the last column of Table 5, shows that all of the introduced palladium (corresponding to 5 wt% in the final catalyst) had been incorporated on the carbon support in each case. Thus, the resulting samples might be used in catalysis (after activation) and be compared directly. It should be noted that for the treated carbon samples, the amount of surface functions present on the surface is in all cases sufficient to graft the totality of the introduced Pd (corresponding to 5 wt% in the final catalyst). It is only in the case of the untreated support (SX+) that the amount of surface functions is slightly too low to guarantee 100% grafting of the Pd; hence some amount of metal might be only adsorbed. However, we believe that we have achieved real grafting of molecular metallic fragments onto the surface of the functionalized carbon supports by the O-groups acting as anchors for the complex precursors. This can be related to recent studies dealing with covalent grafting of coordination compounds on carbon supports [62–66], where the grafted moieties are then used as "intact" fragments for catalysis, which could also be an interesting field of application for the present study. However, we have chosen to use the grafted molecules as precursors for the formation, by thermal activation, of supported metallic particles of controlled size and dispersion, in parallel to another study dealing with the anchoring of $[(C_3H_5)Pd(C_5H_5)]$ onto oxidized diamond to produce small Pd particles via reduction [60].

3.3. Activation of materials

To optimize the activation step, the results from TGA analysis of the starting complex $[Pd(OAc)_2(Et_2NH)_2]$, which showed that the total loss of ligands occurred at 200 °C (after about 20 min), were taken into account. In addition, DRIFTS/MS (Fig. 3) was implemented as an in situ method to follow the departure of ligands during thermal activation. Indeed, heating of functionalized carbon samples grafted with Pd complexes led to desorption of ligands as typical fragments [80], which were observed by mass spectrometry (MS). These MS results confirmed the previously established models: $[Pd(OAc)_2(bipy)]$ grafted on carbon gave rise to fragments only from bipyridine, whereas $[Pd(OAc)_2(Et_2NH)_2]$ gave rise to fragments from both ligands. This in situ DRIFTS/MS characterization of the grafted samples allowed us to follow the desorption of ligands from the surface, starting at 150 °C, confirming the TGA results on the "pure" unsupported complexes. Taking these facts into account, two activation temperatures were selected for comparison: 200 and 500 °C.

First, activation of the grafted samples $[Pd(OAc)_x(Et_2NH)_y]$/C was carried out in a tubular oven under nitrogen flow at 500 °C for 18 h (activation I). The activated catalysts thus obtained were characterized by CO chemisorption (Table 6; Fig. 4); the Pd dispersion values thus obtained increased with the initial carbon acidity in a nonlinear way, reaching a plateau for highly functionalized carbons, whereas the sample modified with H_2O_2 displayed a surprisingly high Pd dispersion value relative to its carbon acidity count. However, the Pd dispersion values were rather low, and the XPS Pd/C ratios before activation were higher than those after activation. Thus, it seemed that the activation step at 500 °C was responsible for agglomeration of palladium atoms on the carbon surface. Indeed, sintering is favored by high temperatures [81]. Moreover, it is known that the oxygenated surface functions of oxidized carbons can be removed by thermal treatment at high temperature, and that the least resistant functions are the carboxylic acid groups [3,6–10], which in this study have been chosen as anchors for the metallic precursor molecules.

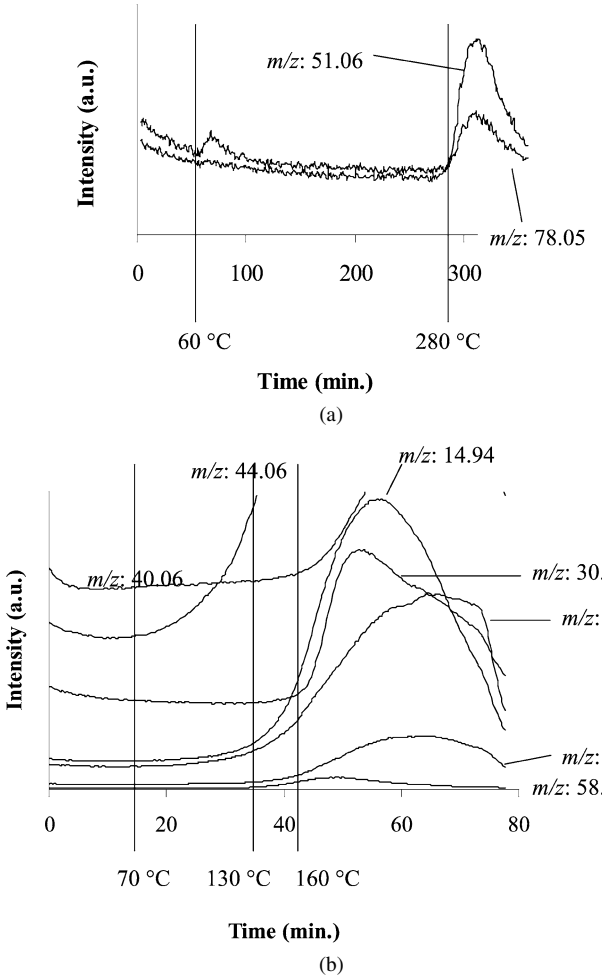

Fig. 3. In situ mass spectrometric characterization of (a) $[Pd(OAc)_2(bipy)]$ and (b) $[Pd(OAc)_2(Et_2NH)_2]$ grafted onto functionalized carbon.

Second, the lower temperature activation was implemented as follows. Activation II was carried out at 200 °C for 4 h, in some cases followed by treatment under hydrogen at 200 °C for 2 h (activation III). This hydrogen treatment was added to ensure complete reduction of Pd, as the catalysts are to be used in a hydrogenation reaction. Characterization of the samples submitted to activations II and III by SEM, XRD (Fig. 5), and CO chemisorption (Table 6) showed that the dispersion was improved compared with that of the samples activated at 500 °C. In particular, the formation of Pd particles of a nonnegligible size (∼25 nm), which were visible by SEM (bright dots in Fig. 5a) and gave rise to sharp X-ray diffraction peaks of Pd (Fig. 5c) for samples activated at 500 °C, was hindered by a lower-temperature activation (less bright dots observed by SEM

Table 6
Pd dispersion measured by CO chemisorption after activation and average particle size in nm (for detail of calculation, see text)

Initial carbon acidity (mmol/100 g C)	After activation I		After activation II		After activation III	
	Pd dispersion (%)	Average particle size (nm)	Pd dispersion (%)	Average particle size (nm)	Pd dispersion (%)	Average particle size (nm)
32.0	2.2	63	–	–	–	–
72.0[a]	3.2	43	–	–	–	–
119.1[a]	4.2	32	–	–	–	–
254.7[a]	5.3	26	13.6	10	17.0	8
52.9[b]	3.8	36	10.8	13	15.3	9

[a] C sample functionalized with HNO_3.
[b] C sample functionalized with H_2O_2.

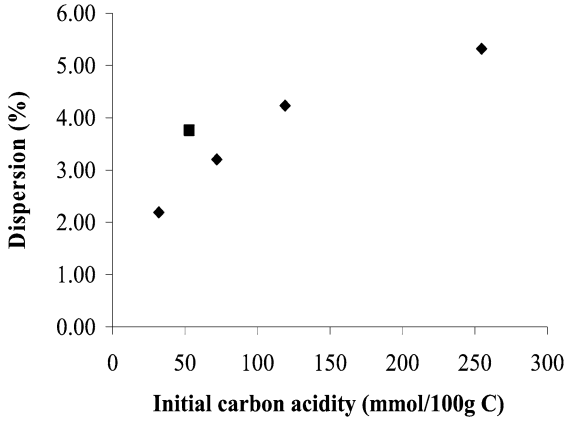

Fig. 4. Evolution of Pd dispersion (after activation I) with initial carbon acidity: (■) carbon modified with H_2O_2, (◆) carbon modified with HNO_3.

but Pd signal by EDXS (see Fig. 5b) and broad Pd XRD peaks (see Fig. 5d)). Moreover, the samples activated under hydrogen (activation III) displayed sharper XPS Pd photopeaks, corresponding, as expected, to a more reduced surface state of the metal. The values of dispersion measured by CO chemisorption (Table 6) allow us to estimate an average particle size, which is 26–63 nm for the samples activated at 500 °C and 8–13 nm for the samples activated at 200 °C, in agreement with SEM characterization. These values of particle sizes were calculated by taking a cubic model for the Pd particles, which gives rise to the following expression: dispersion $= 5/a$, where a = particle size = length of cube edge expressed in number of Pd atoms (we have taken the radius of a Pd atom as 0.137 nm) [82]. The fact that the highest dispersion obtained in this work is only ∼17% can again be ascribed to the thermal fragility of the carboxylic acid functions used as anchors, even at temperatures as low as 200 °C. Indeed, if these functions were destroyed thermally, then metal agglomeration would be favored. Finally, the 5 wt% Pd loading in these samples derived from $[Pd(OAc)_x(Et_2NH)_y]$/C was verified after activation by ICP-AES.

3.4. Catalytic results

To quantify the catalytic performance of the Pd(5 wt%)/C materials obtained from the activated $[Pd(OAc)_x(Et_2NH)_y]$/C, the specific activity in the hydrogenation of 2-methyl-2-nitropropane (MNP) into t-butylamine (TBA) was measured (see Scheme 1). This involved determining the conversion rate of MNP (Table 7). Two intermediates are produced in this reaction—2-methyl-2-nitrosopropane and t-butylhydroxylamine—but the nitroso compound is very reactive and thus accumulates very little [70]. The values of activity obtained here are in the range 1×10^{-3}–3×10^{-3} mol/(L min g), which compares well with the results obtained under similar testing conditions with a commercial Pd(5%)/C catalyst from Johnson Matthey (JM 487), which gave a value of 1.51×10^{-3} (Pd dispersion: 12.3%) [82]. However, much better results were obtained with a Pd(5%)/C catalyst from Degussa (E10N), which gave a value of 8.68×10^{-3} mol/(min g) (Pd dispersion, 11.2%), again under similar experimental conditions. The catalytic results for various samples are also shown in Figs. 6 and 7, as functions of the initial carbon acidity and Pd dispersion, respectively. The specific activity increased linearly with the initial carbon acidity when activation I and HNO_3-modified carbon were used. Activation III gave better performance, as well as H_2O_2-modified carbon. These observations seemed related mainly to an effect of Pd dispersion on the activity (see Fig. 7); however, the H_2O_2-modified carbon still led to a slightly more active catalyst. This must be due not to the number of oxygenated functions introduced initially on the surface, but to their nature, because it has already been shown that they are not innocent in this kind of reaction [70,72]. The O-groups introduced on the carbon support in this study thus played a double role: serving as anchors for the grafting of Pd precursors, thus increasing the dispersion, and playing an active role during the catalytic process that remains to be investigated in greater detail.

Table 7
Catalytic results in terms of conversion rate of MNP

Initial carbon acidity (mmol/100 g)	Activation	Pd dispersion (%)	Activity (mol/(L min g))
32.0	I	2.29	0.00114
72.0	I	3.20	0.00122
254.7	I	5.32	0.00154
231.0	III	17.02	0.00279
52.9[a]	I	3.76	0.00154

[a] C sample functionalized with H_2O_2.

4. Conclusion

In this work, we have shown that it is possible to use a continuous approach for carbon-supported catalyst preparation by

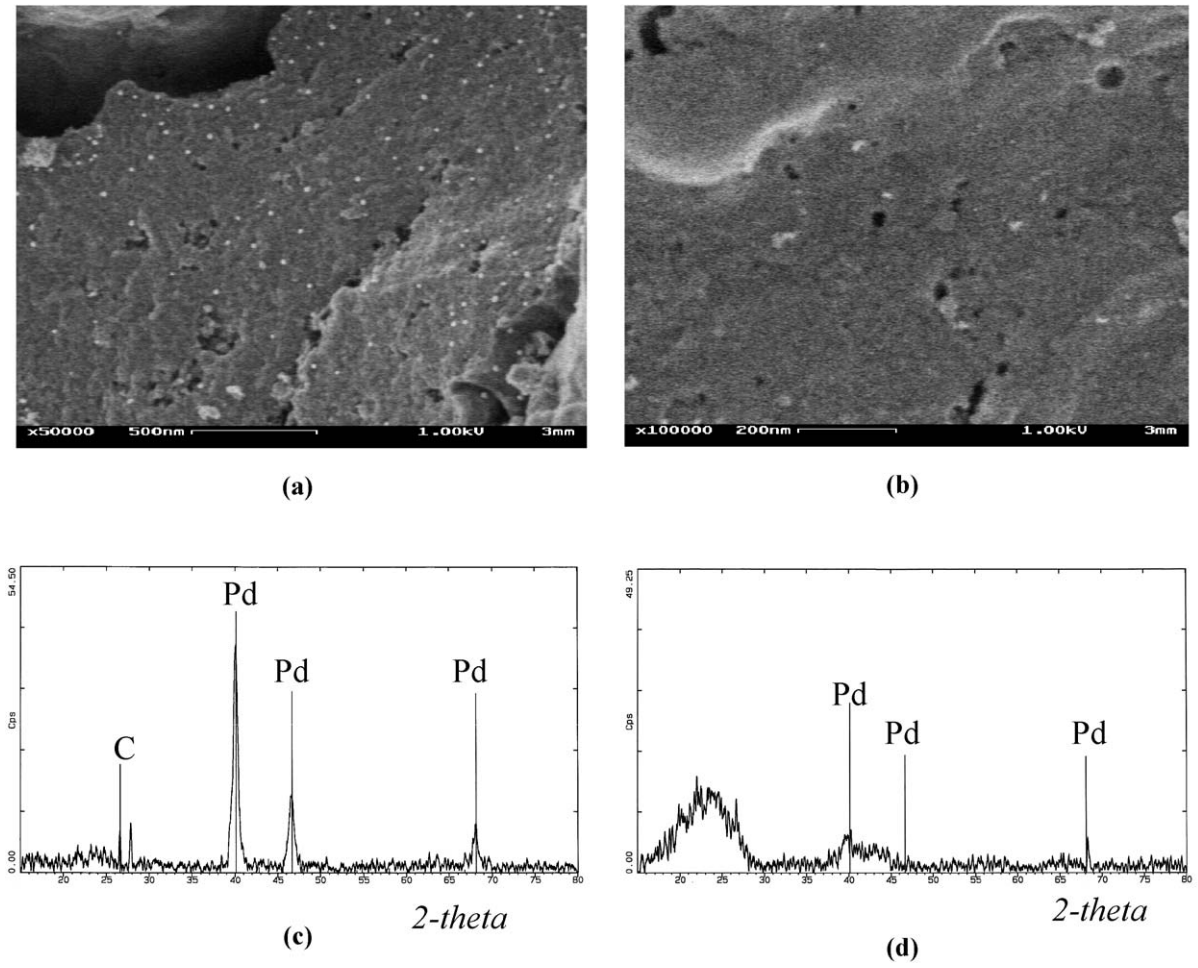

Fig. 5. SEM and XRD characterization of samples activated (a, c) at 500 °C for 18 h and (b, d) at 200 °C for 1 h, and prepared from carbon modified with HNO_3 1 mol/L under reflux for 24 h. Magnification: (a) ×50,000; (b) ×100,000. The vertical lines in the XRD diffractograms correspond to the expected lines for metallic Pd.

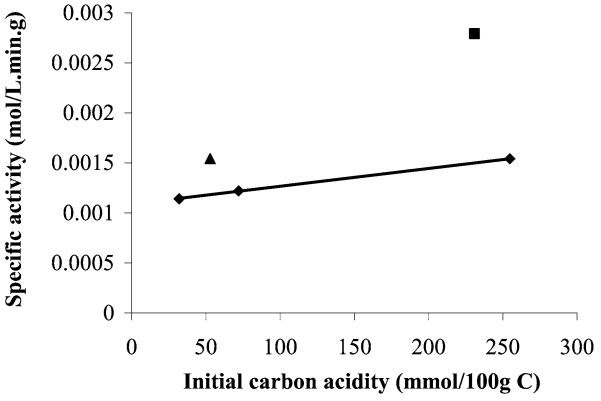

Fig. 6. Evolution of specific activity with initial carbon acidity: (◆) activation I and carbon modified with HNO_3, (■) activation III and carbon modified with HNO_3, (▲) activation I and carbon modified with H_2O_2.

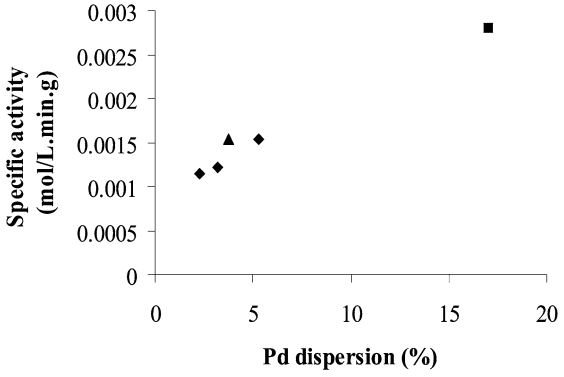

Fig. 7. Evolution of specific activity with Pd dispersion: (◆) activation I and carbon modified with HNO_3, (■) activation III and carbon modified with HNO_3, (▲) activation I and carbon modified with H_2O_2.

developing a controlled methodology for the synthesis of Pd/C materials. We have exploited the possibility offered by carbonaceous materials of modifying the number of surface acid sites, then using these for grafting coordination compounds selected as suitable metallic precursors. The described synthetic procedure was aimed not to develop a commercially viable process, but rather to provide materials that could be characterized at each step of their genesis, thus providing mechanistic insight and room for optimization.

Surface functionalization of SX+ carbon was achieved using HNO_3 or H_2O_2. The amount of oxygenated surface functions introduced, as well as their nature, were determined using Boehm's titration, XPS, and DRIFTS characterization

methods. The nature of the introduced functions was shown to be different for each reactant, and their amount was increased by temperature and concentration. The surface functions were then used as anchors for selected Pd carboxylate complexes of general formula $[Pd(O_2CR)_2(N\text{-ligand})_x]$. The ligand-exchange mechanisms were studied by XPS, and the prevailing models for the grafted fragments were established to be "Pd(bipy)" or "Pd(OAc)(Et_2NH)" when starting from $[Pd(O_2CCR_3)_2(bipy)]$ or $[Pd(OAc)_2(Et_2NH)_2]$, respectively. Monometallic Pd(5 wt%)/C catalysts were prepared by grafting $[Pd(OAc)_2(Et_2NH)_2]$ onto various samples of functionalized carbon. The activation step was optimized (temperature and duration) on the basis of TGA and MS analyses to give well-dispersed samples, which were characterized by XRD, SEM, and CO chemisorption. The catalytic performance in the hydrogenation of MNP for HNO_3-modified samples was related to the initial carbon acidity (for selected activation conditions) and to Pd dispersion (whatever the activation conditions), whereas they were unexpectedly improved for H_2O_2-modified samples, probably due to the different types of oxygenated surface functions introduced (or variable ratios of the same types), which are thought to play an active role in the catalytic process besides serving as anchors during catalyst preparation.

Acknowledgments

The authors thank R. Rozenberg and J.-L. Habib Jiwan for mass spectrometric characterization of the carboxylate complexes and useful discussions, A. Iserentant for help with metal loading determinations, J.-F. Statsyns for technical support, and D. Desmecht and P. Verhasselt for assistance during the catalytic tests. The NORIT firm is also acknowledged for supplying the SX+ carbon support. Financial support was provided by the Belgian National Fund for Scientific Research (FNRS) and the Communauté Française de Belgique (through an "ARC" concerted research program). Moreover, O.D. acknowledges financial support from the "Concorde" package (EC-funded) and the Belgian FRIA.

References

[1] R. Schlögl, Handbook of Heterogeneous Catalysis, VCH, 1997, Ch. 2.
[2] E. Auer, A. Freund, J. Pietsch, T. Tacke, Appl. Catal. A 173 (1998) 259.
[3] A. Polania, E. Papirer, J.B. Donnet, G. Dagois, Carbon 31 (1993) 473.
[4] A. Ahmadpour, D.D. Do, Carbon 34 (1996) 471.
[5] C. Moreno-Castilla, J. Rivera-Utrilla, MRS Bull. 26 (2001) 890.
[6] G. de la Puente, J.J. Pis, J.A. Menendez, P. Grange, J. Anal. Appl. Pyrol. 43 (1997) 125.
[7] C. Moreno-Castilla, F. Carrasco-Marin, F.J. Maldonado-Hodar, J. Rivera-Utrilla, Carbon 36 (1998) 145.
[8] J.L. Figueiredo, M.F.R. Pereira, M.M.A. Freitas, J.J.M. Orfao, Carbon 37 (1999) 1379.
[9] M.A. Fraga, M.J. Mendes, E. Jordao, J. Mol. Catal. A Chem. 179 (2002) 243.
[10] P.C.C. Faria, J.J.M. Orfao, M.F.R. Pereira, Water Res. 38 (2004) 2043.
[11] H.P. Boehm, Carbon 32 (1994) 759.
[12] P. Ehrburger, O.P. Mahajan, P.L. Walker, J. Catal. 43 (1976) 61.
[13] D.J. Suh, T.J. Park, S.K. Ihm, Carbon 31 (1993) 427.
[14] Y. Otake, R.G. Jenkins, Carbon 31 (1993) 109.
[15] E. Papirer, R. Lacroix, J.-B. Donnet, Carbon 34 (1996) 1521.
[16] H.-P. Boehm, E. Diehl, W. Heck, R. Sappok, Angew. Chem. Int. Ed. 3 (1964) 669.
[17] R.C. Sosa, R.F. Parton, P.E. Neys, O. Lardinois, P.A. Jacobs, P.G. Rouxhet, J. Mol. Catal. A Chem. 110 (1996) 141.
[18] G. Farkas, L. Hegedus, A. Tungler, T. Mathe, J.L. Figueiredo, M. Freitas, J. Mol. Catal. A Chem. 153 (2000) 215.
[19] M. Gurrath, T. Kuretzky, H.P. Boehm, L.B. Okhlopkova, A.S. Lisitsyn, V.A. Likholobov, Carbon 38 (2000) 1241.
[20] A.E. Aksoylu, M. Madalena, A. Freitas, M.F.R. Pereira, J.L. Figueiredo, Carbon 39 (2001) 175.
[21] M.A. Fraga, E. Jordao, M.J. Mendes, M.M.A. Freitas, J.L. Faria, J.L. Figueiredo, J. Catal. 209 (2002) 355.
[22] P.E. Fanning, M.A. Vannice, Carbon 31 (1993) 721.
[23] M. Domingo-Garcia, F.J. Lopez-Garzon, M. Perez-Mendoza, J. Colloid Interface Sci. 222 (2000) 233.
[24] M. Perez-Mendoza, M. Domingo-Garcia, F.J. Lopez-Garzon, Appl. Catal. A 224 (2002) 239.
[25] F.J. Lopez-Garzon, M. Domingo-Garcia, M. Perez-Mendoza, P.M. Alvarez, V. Gomez-Serrano, Langmuir 19 (2003) 2838.
[26] G.C. Torres, E.L. Jablonski, G.T. Baronetti, A.A. Castro, S.R. de Miguel, O.A. Scelza, M.D. Blanco, M.A.P. Jimenez, J.L.G. Fierro, Appl. Catal. A 161 (1997) 213.
[27] C. Moreno-Castilla, M.A. Ferro-Garcia, J.P. Joly, I. Bautista-Toledo, F. Carrasco-Marin, J. Rivera-Utrilla, Langmuir 11 (1995) 4386.
[28] C. Moreno-Castilla, F. Carrasco-Marin, A. Mueden, Carbon 35 (1997) 1619.
[29] B.K. Pradhan, N.K. Sandle, Carbon 37 (1999) 1323.
[30] M. Santiago, F. Stuber, A. Fortuny, A. Fabregat, J. Font, Carbon 43 (2005) 2134.
[31] P. Vinke, M. Vandereijk, M. Verbree, A.F. Voskamp, H. Vanbekkum, Carbon 32 (1994) 675.
[32] M. Acedo-Ramos, V. Gomez-Serrano, C. Valenzuela-Calahorro, A.J. Lopez-Peinado, Spectrosc. Lett. 26 (1993) 1117.
[33] H.-P. Boehm, Angew. Chem. Int. Ed. 5 (1966) 533.
[34] C.A.L.Y. Leon, L.R. Radovic, Chem. Phys. Carb. 24 (1994) 213.
[35] J.M. O'Reilly, R.A. Mosher, Carbon 21 (1983) 47.
[36] I.I. Salame, T.J. Bandosz, J. Colloid Interface Sci. 240 (2001) 252.
[37] K. Laszlo, K. Josepovits, E. Tombacz, Anal. Sci. 17 (2001) il741.
[38] M. Domingo-Garcia, F.J.L. Garzon, M.J. Perez-Mendoza, J. Colloid Interface Sci. 248 (2002) 116.
[39] T. Cordero, J. Rodriguez-Mirasol, N. Tancredi, J. Piriz, G. Vivo, J.J. Rodriguez, Ind. Eng. Chem. Res. 41 (2002) 6042.
[40] J.S. Noh, J.A. Schwarz, Carbon 28 (1990) 675.
[41] J.M. Solar, C.A.L. Leon, K. Osseoasare, L.R. Radovic, Carbon 28 (1990) 369.
[42] V. Strelko, D.J. Malik, J. Colloid Interface Sci. 250 (2002) 213.
[43] A.N.A. El-Hendawy, Carbon 41 (2003) 713.
[44] G. Soto-Garrido, C. Aguilar, R. Garcia, R. Arriagada, J. Chil. Chem. Soc. 48 (2003) 65.
[45] J.Y. Li, L. Ma, X.N. Li, C.S. Lu, H.Z. Liu, Ind. Eng. Chem. Res. 44 (2005) 5478.
[46] S.S. Barton, M.J.B. Evans, E. Halliop, J.A.F. MacDonald, Carbon 35 (1997) 1361.
[47] B. Milani, E. Alessio, G. Mestroni, A. Sommazzi, F. Garbassi, E. Zangrando, N. Brescianipahor, L. Randaccio, J. Chem. Soc. Dalton Trans. (1994) 1903.
[48] N. Krishnankutty, M.A. Vannice, Chem. Mater. 7 (1995) 754.
[49] H. Tamon, M. Okazaki, Carbon 34 (1996) 741.
[50] A. Gil, G. de la Puente, P. Grange, Micropor. Mater. 12 (1997) 51.
[51] J. Choma, W. Burakiewicz-Mortka, M. Jaroniec, Z. Li, J. Klinik, J. Colloid Interface Sci. 214 (1999) 438.
[52] V. Dubois, Y. Dal, G. Jannes, Stud. Surf. Sci. Catal. 143 (2002) 993.
[53] L. Calvo, M.A. Gilarranz, J.A. Casas, A.F. Mohedano, J.J. Rodriguez, Ind. Eng. Chem. Res. 44 (2005) 6661.
[54] E. Ahumada, H. Lizama, F. Orellana, C. Suarez, A. Huidobro, A. Sepulveda-Escribano, F. Rodriguez-Reinoso, Carbon 40 (2002) 2827.

[55] M.F.R. Pereira, S.F. Soares, J.J.M. Orfao, J.L. Figueiredo, Carbon 41 (2003) 811.
[56] C. Prado-Burguete, A. Linares-Solano, F. Rodriguez-Reinoso, C.S. Delecea, J. Catal. 115 (1989) 98.
[57] V. Gomez-Serrano, M. Acedo-Ramos, A.J. Lopez-Peinado, C. Valenzuela-Calahorro, Fuel 73 (1994) 387.
[58] N. Krishnankutty, M.A. Vannice, J. Catal. 155 (1995) 312.
[59] P.C. L'Argentiere, E.A. Cagnola, D.A. Liprandi, M.C. Roman-Martnez, C.S.M. de Lecea, Appl. Catal. A 172 (1998) 41.
[60] Y.A. Ryndin, O.S. Alekseev, P.A. Simonoc, V.A. Likholobov, J. Mol. Catal. 55 (1989) 109.
[61] A. Aramata, S. Takahashi, G.P. Yin, Y.Z. Gao, Y. Inose, H. Mihara, A. Tadjeddine, W.Q. Zheng, O. Pluchery, A. Bittner, A. Yamagishi, Thin Solid Films 424 (2003) 239.
[62] A.R. Silva, M. Martins, M.M.A. Freitas, J.L. Figueiredo, C. Freire, B. de Castro, Eur. J. Inorg. Chem. (2004) 2027.
[63] A.R. Silva, J.L. Figueiredo, C. Freire, B. de Castro, Catal. Today 102 (2005) 154.
[64] B. Jarrais, A.R. Silva, C. Freire, Eur. J. Inorg. Chem. (2005) 4582.
[65] A.R. Silva, V. Budarin, J.H. Clark, B. de Castro, C. Freire, Carbon 43 (2005) 2096.
[66] A. Valente, A.M.B. do Rego, M.J. Reis, I.F. Silva, A.M. Ramos, J. Vital, Appl. Catal. A 207 (2001) 221.
[67] D.C. Iffland, F.A. Cassis, J. Am. Chem. Soc. 74 (1952) 6284.
[68] GB Patent 925,458 to Engelhard Industries (1963).
[69] G. Carturan, G. Facchin, G. Cocco, G. Navazio, G. Gubitosa, J. Catal. 82 (1983) 56.
[70] V. Dubois, G. Jannes, P. Verhasselt, Stud. Surf. Sci. Catal. 108 (1997) 263.
[71] F.J. Derbyshire, V.H.J. de Beer, G.M.K. Abotsi, A.W. Scaroni, J.M. Solar, D.J. Skrovanek, Appl. Catal. 27 (1986) 117.
[72] N. Bouchenafa-Saib, P. Grange, P. Verhasselt, F. Addoun, V. Dubois, Appl. Catal. A 286 (2005) 167.
[73] J.M. Solar, F.J. Derbyshire, V.H.J. Debeer, L.R. Radovic, J. Catal. 129 (1991) 330.
[74] S. Hermans, M. Wenkin, M. Devillers, J. Mol. Catal. A Chem. 136 (1998) 59.
[75] T.A. Stephenson, S.M. Morehouse, A.R. Powell, J.P. Heffer, G. Wilkinson, J. Chem. Soc. (1965) 3632.
[76] L. Soptrajanova, B. Soptrajanov, Spectrosc. Lett. 25 (1992) 1141.
[77] M.L. Toebes, E.M.P. van Heeswijk, J.H. Bitter, A.J. van Dillen, K.P. de Jong, Carbon 42 (2004) 307.
[78] G.B. Deacon, R.J. Phillips, Coord. Chem. Rev. 33 (1980) 227.
[79] S.V. Kravtsova, I.P. Romm, A.I. Stash, V.K. Belsky, Acta Crystallogr. Sect. C 52 (1996) 2201.
[80] SDBS Web database, National Institute of Advanced Industrial Science and Technology, Japan, 2006; http://www.aist.go.jp/RIODB/SDBS/.
[81] J.J. Chen, E. Ruckenstein, J. Catal. 69 (1981) 254.
[82] V. Dubois, Ph.D. thesis, Institut Meurice (Brussels) and Université catholique de Louvain (Louvain-la-Neuve), Belgium, 2000.